

# Design of steel frames by an enhanced moth-flame optimization algorithm

Saeed Gholizadeh<sup>\*</sup>, Hamed Davoudi<sup>a</sup> and Fayegh Fattahi<sup>b</sup>

Department of Civil Engineering, Urmia University, Urmia, West Azerbaijan Province, Iran

(Received October 11, 2016, Revised February 22, 2017, Accepted March 16, 2017)

**Abstract.** Structural optimization is one of the popular and active research areas in the field of structural engineering. In the present study, the newly developed moth-flame optimization (MFO) algorithm and its enhanced version termed as enhanced moth-flame optimization (EMFO) are employed to implement the optimization process of planar and 3D steel frame structures with discrete design variables. The main inspiration of this optimizer is the navigation method of moths in nature called transverse orientation. A number of benchmark steel frame optimization problems are solved by the MFO and EMFO algorithms and the results are compared with those of other meta-heuristics. The obtained numerical results indicate that the proposed EMFO algorithm possesses better computational performance compared with other existing meta-heuristics.

**Keywords:** steel structures; optimization; meta-heuristic; enhanced moth-flame algorithm

## 1. Introduction

Structural optimization aims to design structures with minimum weight, or minimize an objective function corresponding to minimal cost of the structures, while the corresponding design constraints are satisfied. Optimization of steel frame structures having many design variables is a computationally difficult task and to tackle it an efficient optimization algorithm should be utilized. Many of gradient-based optimization algorithms have difficulties when dealing with such type of problems and they may converge to local optima. In the recent decades, a number of meta-heuristic algorithms have been developed based on natural phenomena. Meta-heuristics have impressive features that differs them from the existing gradient-based methods. This class of optimization techniques not only requires no gradient computations but also they are simple for computer programming and implementation. The efficiency of meta-heuristics derives from the fact that they are designed to imitate the best features in nature inspiring to different sources. Biological systems are the main source for proposing new nature-inspired meta-heuristics because the selection of the fittest in biological systems has evolved by natural selection over millions of years (Talatahari *et al.* 2015). The meta-heuristics demonstrate their efficiency in tackling complex problems and this is why they have been widely employed in the field of structural optimization.

Many researchers employed different meta-heuristic algorithms for optimal design of steel structures. Gholizadeh and Poorhoseini (2015) proposed a modified Dolphin echolocation (MDE) algorithm in which the step

locations are determined using one-dimensional chaotic maps. Artar and Daloğlu (2015) utilized a method based on genetic algorithm (GA) for minimum weight design of steel frames containing composite beams, semi-rigid connections and column bases. Aydin *et al.* (2015) presented an algorithm to attain the optimal distribution of steel diagonal bracings in planar steel frames using artificial bee colony (ABC) algorithm. Kaveh and Shokohi (2015) employed colliding bodies optimization (CBO) meta-heuristic to find optimal design of laterally-supported castellated steel beams. Kaveh and Bakhshpoori (2015) presented subspace search mechanism (SSM) to reduce the computational time for convergence of cuckoo search algorithm (CSA) for size optimization of truss structures. Gholizadeh and Barati (2014) applied a hybrid firefly algorithm (FA) and particle swarm optimization (PSO) for topology optimization of geometrically nonlinear single layer steel domes. Rafiee *et al.* (2013) developed the big bang-big crunch (BB-BC) meta-heuristic algorithm for optimal design of non-linear steel frames with semi-rigid beam-to-column connections.

One of the popular structural optimization problems is frame structure design for minimum weight and to efficiently address the problem, application of new optimization algorithms or some modifications to the existing ones are often required. Therefore, researchers have attempted to solve frame structures as a real-world, discrete-variable and nonlinear optimization problem using different methods (Lamberti and Pappalettere 2011). In this field, GA (Pezeshk *et al.* 2000), ant colony optimization (ACO) (Camp *et al.* 2005), harmony search (HS) (Degertekin 2008), improved ant colony optimization (IACO) (Kaveh and Talatahari 2010), evolution strategy (ES) (Hasancebi *et al.* 2011), teaching-learning based optimization (TLBO) (Togan 2012) and modified particle swarm optimization (MPSO) (Gholizadeh and Fattahi 2014) have been employed to design of steel frames. In this work, the newly developed moth-flame optimization (MFO)

\*Corresponding author, Ph.D., Associate Professor,  
E-mail: [s.gholizadeh@urmia.ac.ir](mailto:s.gholizadeh@urmia.ac.ir)

<sup>a</sup> Structural Engineer

<sup>b</sup> Ph.D. Student

algorithm (Mirjalili 2015) is employed to implement optimization of steel frame structures. MFO is designed based on the navigation method of natural moths termed as transverse orientation. Moths fly in night by maintaining a fixed angle with respect to the moon, a very effective mechanism for travelling in a straight line for long distances. However, these fancy insects are trapped in a useless spiral path around artificial lights. As compared to other robust design optimization methods, MFO is more efficient, requiring fewer number of function evaluations, while leading to better or the same quality of results (Mirjalili 2015). However, the numerical results of this study reveal that MFO is not suitable for solving the discrete optimization problems of steel frame structures with large design spaces. Therefore, an enhanced moth-flame optimization (EMFO) algorithm is proposed in the present study to tackle this class of complex structural optimization problems. Three benchmark steel structure optimization problems including a ten-story and a twenty four-story planar steel frames and a twenty-story 3D steel braced frame are solved by MFO and EMFO algorithms and the obtained results are compared with those of the GA, ACO, HS, IACO, ES, TLBO and MPSO meta-heuristics. In these problems, the design variables are cross-sections of the structural elements and the design constraints are imposed on the nodal displacements and element stresses. The numerical results demonstrate the efficiency of the proposed EMFO in comparison with MFO and other meta-heuristic algorithms.

In the present work, in order to evaluate the necessary structural responses during the optimization process, ANSYS platform (2006) is employed. Furthermore, all of the required computer programs for implementation of optimization process by MFO and EMFO algorithms are coded in MATLAB (2006) platform. For computer implementation a system with Core™2 Duo 2.66 GHz CPU is employed.

## 2. Optimization problem formulation

The optimization problem of a steel frame including  $ne$  members collected in  $ng$  design groups can be formulated as follows

$$\text{Find: } X = \{x_1 \ x_2 \ \dots \ x_i \ \dots \ x_{ng}\}^T \quad (1)$$

$$\text{To minimize: } f(X) = \sum_{i=1}^{ng} \rho_i A_i \sum_{j=1}^{nm} L_j \quad (2)$$

$$\text{Subject to: } g_k(X) \leq 0, \quad k = 1, 2, \dots, nc \quad (3)$$

where  $x_i$  is an integer value expressing the sequence numbers of steel sections assigned to  $i$ th group;  $f$  represents the weight of the frame,  $\rho_i$  and  $A_i$  are weight of unit volume and cross-sectional area of the  $i$ th group section, respectively;  $nm$  is the number of elements collected in the  $i$ th group;  $L_j$  is the length of the  $j$ th element in the  $i$ th group;  $g_k$  is the  $k$ th constraint.

The lateral displacement and inter-story drift constraints

are usually taken as

$$g_\delta = \frac{(\delta/H)}{R} - 1 \leq 0 \quad (4)$$

$$g_l = \frac{(d_l/h_l)}{R_l} - 1 \leq 0, \quad l = 1, \dots, ns \quad (5)$$

where  $\delta$  is the maximum lateral displacement;  $H$  is the height of the frame structure;  $R$  is the maximum drift index;  $d_l$  is the inter-story drift;  $h_l$  is the story height of the  $l$ th floor;  $ns$  is the total number of stories; and  $R_l$  is the inter-story drift index permitted by the code of practice.

The demand-capacity ratio (DCR) constraints for structural elements subjected to axial and flexural stresses are computed as follows:

If the code of practice is selected ASD-AISC (1989), Eqs. (6) and (7) should be used. For the flexural members under tension, the second part of Eq. (6) should be used

$$\text{for } \frac{f_a}{F_a} > 0.15$$

$$g_{DCR} = \begin{cases} \left[ \frac{f_a}{F_a} + \frac{C_{mx} f_{bx}}{\left(1 - \frac{f_a}{F'_{ex}}\right) F_{bx}} + \frac{C_{my} f_{by}}{\left(1 - \frac{f_a}{F'_{ey}}\right) F_{by}} \right] - 1 \leq 0 \\ \left[ \frac{f_a}{0.6F_y} + \frac{f_{bx}}{F_{bx}} + \frac{f_{by}}{F_{by}} \right] - 1 \leq 0 \end{cases} \quad (6)$$

$$\text{for } \frac{f_a}{F_a} \leq 0.15$$

$$g_{DCR} = \left[ \frac{f_a}{F_a} + \frac{f_{bx}}{F_{bx}} + \frac{f_{by}}{F_{by}} \right] - 1 \leq 0 \quad m = 1, \dots, ne \quad (7)$$

In which  $f_a$  represents the computed axial stress;  $f_{bx}$  and  $f_{by}$  are the computed flexural stresses due to bending of the member about its major ( $x$ ) and minor ( $y$ ) principal axes, respectively.  $F'_{ex}$  and  $F'_{ey}$  are the Euler stresses about principal axes of the member;  $F_a$  represent the allowable axial stress under axial compression force alone, and is calculated depending on elastic or inelastic buckling failure mode of the member using ASD-AISC (1989). The allowable bending compressive stresses about major and minor axes are designated by  $F_{bx}$  and  $F_{by}$ ;  $C_{mx}$  and  $C_{my}$  are the reduction factors, introduced to counterbalance overestimation of the effect of secondary moments. Also,  $F_y$  is the material yield stress.

If the code of practice is selected LRFD-AISC (2001), Eqs. (8) and (9) should be used

$$\text{for } \frac{P_u}{\Phi_c P_n} < 0.2$$

$$g_{DCR} = \left[ \frac{P_u}{2\Phi_c P_n} + \left( \frac{M_{ux}}{\Phi_b M_{nx}} + \frac{M_{uy}}{\Phi_b M_{ny}} \right) \right] - 1 \leq 0 \quad (8)$$

$$\text{for } \frac{P_u}{\Phi_c P_n} > 0.2$$

$$g_{DCR,m} = \left[ \frac{P_u}{\Phi_c P_n} + \frac{8}{9} \left( \frac{M_{ux}}{\Phi_b M_{nx}} + \frac{M_{uy}}{\Phi_b M_{ny}} \right) \right] - 1 \leq 0 \quad (9)$$

$$m = 1, \dots, ne$$

where  $P_u$  is the required strength (tension or compression);  $P_n$  is the nominal axial strength (tension or compression);  $\Phi_c$  is the resistance factor;  $M_{ux}$  and  $M_{uy}$  are the required flexural strengths in the  $x$  and  $y$  directions; respectively;  $M_{nx}$  and  $M_{ny}$  are the nominal flexural strengths in the  $x$  and  $y$  directions; and  $\Phi_b$  is the flexural resistance reduction factor.

In order to satisfy practical demands, geometric constraints should be considered in beam-column framing joints for 2D frames as follows

$$g_B = \frac{b_{fb}}{b_{fc}} - 1 \leq 0 \quad (10)$$

$$g_C = \left\{ \begin{array}{l} b_f^{TC} \\ b_f^{BC} - 1 \leq 0, \quad d^{TC} \\ d^{BC} - 1 \leq 0 \end{array} \right\} \quad n = 1, \dots, nj \quad (11)$$

where  $b_{fb}$  and  $b_{fc}$  are the flange width of beam and column, respectively;  $b_f^{TC}$  and  $b_f^{BC}$  are the flange width of the top and bottom columns, respectively;  $d^{TC}$  and  $d^{BC}$  are the depth of the top and bottom columns, respectively;  $nj$  is the number of joints.

In the present work, the exterior penalty function method (EPPM) is employed to handle the design constraints. The EPPM transforms the basic constrained optimization problem into the unconstrained formulation. In this case, the pseudo unconstrained objective function (PUOF) can be represented as follows

$$\Psi(X, r_p) = f(X) (1 + r_p P(X)) \quad (12)$$

$$P(X) = \sum_{k=1}^{nc} (\max\{0, g_k(X)\})^2 \quad (13)$$

where  $\Psi(X, r_p)$ ,  $P(X)$  and  $r_p$  are the PUOF, penalty function, and a penalty parameter, respectively. In this study,  $r_p$  is linearly increased from 1.0 at the first iteration to  $10^6$  at the last one during the optimization process.

For minimizing the above pseudo objective function, MFO algorithm and its enhanced version are employed in the present study. The theoretical backgrounds of these meta-heuristics are explained in the next sections.

### 3. Moth-flame optimization algorithm

Moths utilize special navigation methods, termed as transverse orientation (TO), to fly in night by maintaining a fixed angle with respect to the moon. In other words, the TO navigation method is only efficient for flying in straight line when the light source is very far. When moths are tricked by a human-made artificial light, they fly spirally

around the light. In fact, they try to maintain a similar angle with the light to fly in straight line. Since such a light is extremely close compared to the moon, however, maintaining a similar angle to the light source causes a deadly spiral fly path for moths. In this case, the moth eventually converges towards the light and this behavior has been modeled mathematically to propose moth-flame optimization (MFO) algorithm by Mirjalili (2015).

In the framework of MFO algorithm, there are two key components: moths ( $X$ ) and flames ( $F$ ). Both of them are solutions of the optimization problem at hand and the difference between them lays in their updating method employed during the optimization process. The moths are actual search agents that move around the search space, whereas flames are the best position of moths that obtains so far. Therefore, each moth searches around a flame and updates it in case of finding a better solution. With this mechanism, a moth never loses its best solution. The fundamental steps of the MFO algorithm are as follows (Mirjalili 2015):

- (1) A swarm including  $n$  moths is generated in an  $m$ -dimensional design space.

$$X = \begin{bmatrix} x_{1,1} & x_{1,2} & \dots & x_{1,n} \\ x_{2,1} & x_{2,2} & \dots & x_{2,n} \\ \vdots & \vdots & \dots & \vdots \\ x_{m,1} & x_{m,2} & \dots & x_{m,n} \end{bmatrix} \quad (14)$$

- (2) The objective function ( $OF$ ) is evaluated for all moths.

$$OF = \{OF_1 \quad OF_2 \quad \dots \quad OF_n\} \quad (15)$$

- (3) The positions of flames are defined by simply sorting moths' positions. So the dimensions of  $M$  and  $F$  arrays are equal at first.

$$F = \text{sort}(X) \quad (16)$$

- (4) The distance between the moths and flames are calculated.

$$D_i = |F_j - X_i| \quad (17)$$

where  $X_i$  indicates the  $i$ th moth and  $F_j$  represents the  $j$ th flame.

- (5) The position of  $i$ th moth is updated with respect to the  $j$ th flame as follows

$$X_i^{\text{new}} = D_i \cdot e^{bt} \cdot \cos(2\pi t) + F_j \quad (18)$$

where  $b$  is a constant to define the shape of the logarithmic spiral,  $t$  is a random number in  $[r, 1]$  and  $r$  is linearly decreased from -1 to -2 during the optimization process.

Eq. (18) allows a moth to fly around a flame and not necessarily in the space between them. Therefore, the exploration and exploitation of the search space can be guaranteed. In the framework of MFO, exploration occurs

when the next position is outside the space between the moth and flame and exploitation happens when the next position lies inside the space between the moth and flame. In order to prevent the algorithm from being prematurely trapped in local optima, each moth is obliged to update its position using only one of the flames in Eq. (18). In each iteration and after updating the list of flames, the flames are sorted based on their fitness values. The moths then update their positions with respect to their corresponding flames. The first moth always updates its position with respect to the best flame, whereas the last moth updates its position with respect to the worst flame (Mirjalili 2015). This means that the first moth selects the first flame, the second moth selects the second flame and consequently the last moth selects the last flame.

As updating the position of moths with respect to  $n$  different locations in design space may degrade the exploitation ability of the algorithm, in the framework of MFO an adaptive mechanism is utilized to determine the number of flames ( $NF$ ) as follows

$$NF = \text{round} \left( n - (n-1) \cdot \frac{itr}{itr_{\max}} \right) \quad (19)$$

where  $itr$  and  $itr_{\max}$  are the current and maximum numbers of iterations, respectively.

#### 4. Enhanced moth-flame optimization algorithm

Computational experiences of the present study indicate that standard MFO is not able to efficiently tackle the optimization problem of steel frame structures with discrete design variables and the algorithm converges to local optima. In the present work, in order to improve the MFO to get more reliable solutions, a modified version of this algorithm, termed here as enhanced moth-flame (EMFO) meta-heuristic algorithm, is proposed.

As the first modification, the best information derived by the swarm during the previous iterations, is effectively involved in the framework of the proposed EMFO to generate a new swarm. To achieve this goal, a new term containing the best position attained so far, is added to the position updating equation of moths as follows

$$X_i^{\text{new}} = D_i \cdot e^{bt} \cdot \cos(2\pi) + F_j + \alpha \cdot r \cdot (X_{\text{best}} - X_i) \quad (20)$$

where  $\alpha$  is a scaling factor which its best value should be determined by performing sensitivity analysis,  $X_{\text{best}}$  is the best position obtained up to current iteration, and  $r$  is a random number in interval  $[0, 1]$ .

As the second modification, a mutation operator is utilized to escape from local optima. For this purpose, a parameter like  $\beta$  within  $(0, 1)$  is introduced and it is specified whether a component of each moth must be changed or not. For each moth,  $\beta$  is compared with  $rn_i$  ( $i = 1, \dots, n$ ) which is a random number uniformly distributed within  $(0, 1)$ . If  $rn_i < \beta$ , one dimension of the  $i$ th moth is selected randomly and its value is regenerated in interval [lower bound, upper bound]. In order to preserve the

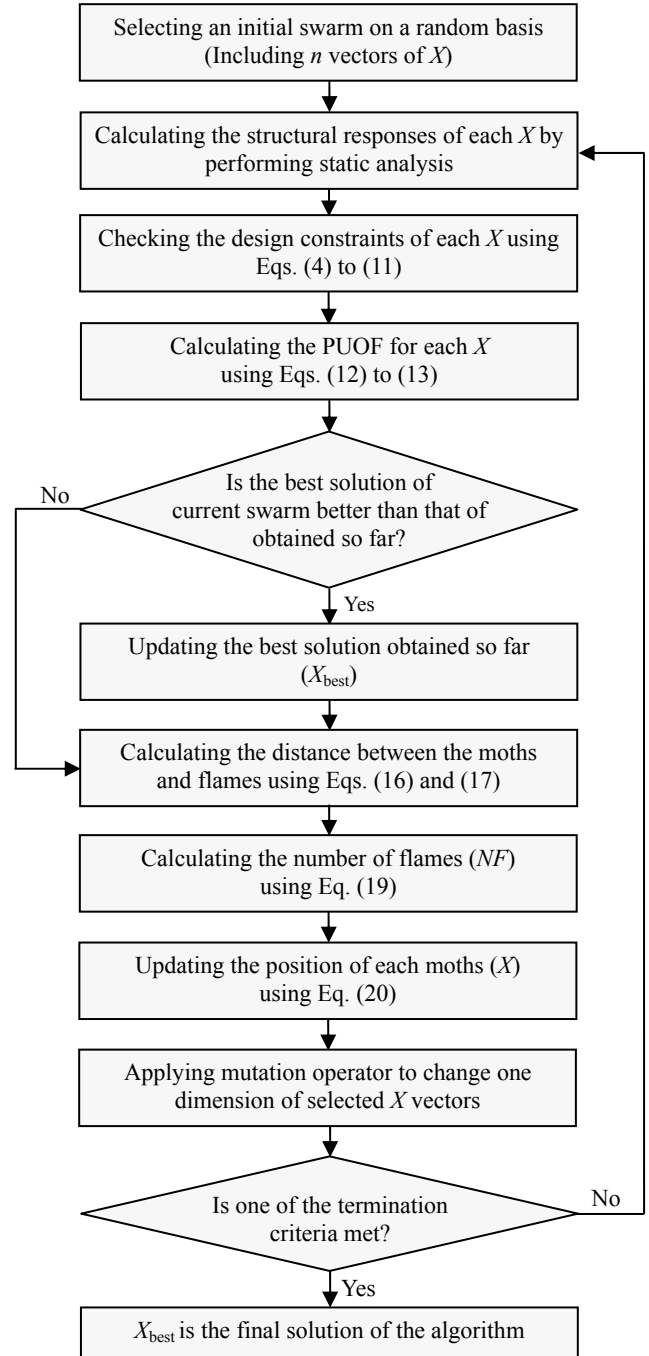


Fig. 1 Flowchart of the proposed EMFO algorithm for optimization of steel frames

structure of swarm, only one design variable is mutated for the selected moths. In the framework of EMFO, the value of  $\beta$  is determined by performing sensitivity analysis.

Fig. 1 shows the flowchart of EMFO for solving the optimization problem of steel frames.

#### 5. Numerical results

In order to investigate the computational performance of the proposed algorithm three benchmark steel frame optimization problems are presented and the results are

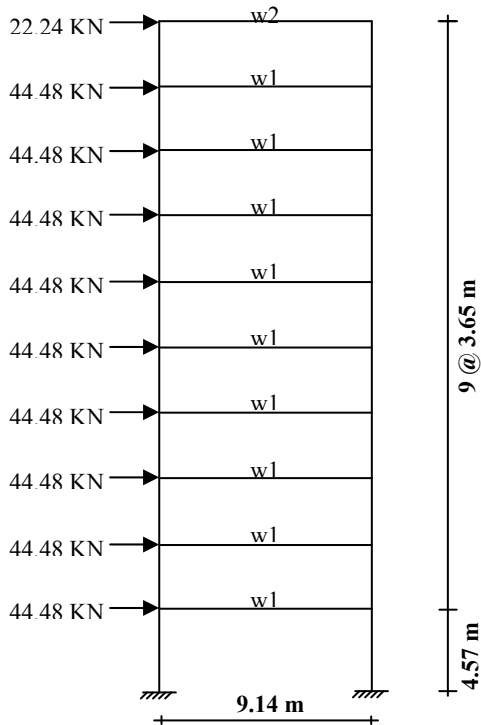


Fig. 2 Ten-story planar steel frame

compared with those of reported in literature.

For all presented design examples, the cross-sections of all members are selected from the standard W-shaped profile list.

In order to find the best setting of internal parameters  $\alpha$  and  $\beta$  for EMFO algorithm, a set of sensitivity analysis is conducted for each example considering the values of 0.25, 0.50, 0.75, 1.00, and 1.50 for  $\alpha$  and 0.2, 0.3, 0.4, and 0.5 for  $\beta$ . For each combination of  $\alpha$  and  $\beta$  parameters 20 independent optimization runs are implemented by EMFO algorithm and the combination leading to the best weight is considered as the optimal setting of the parameters.

### 5.1 One-bay ten-story planar steel frame

Fig. 2 shows the topology and the loading conditions for a ten-story steel frame. The effective length factors of the members are calculated as  $K_x \geq 1.0$  for a sway-permitted frame and the out-of-plane effective length factor is specified as  $K_y = 1$ . In this example,  $E = 200$  GPa and  $F_y = 248.2$  MPa. In Fig. 2, w1 and w2 are 87.56 and 43.78 kN/m, respectively.

Each column is considered un-braced along its length, and the un-braced length for each beam member is specified as one-fifth of the span length. Fabrication conditions are imposed on the construction of the elements of frame requiring the same beam section to be used for three consecutive stories, beginning at the foundation, and that the same column section is used every two consecutive stories. The element grouping results in four beam sections and five column sections for a total of nine design variables. The cross-section of the all beam element groups are chosen from all 267 W-shaped sections, while the column sections

Table 1 The results of sensitivity analysis for ten-story planar steel frame

No.	$\alpha$	$\beta$	Best weight (kN)
1	0.25	0.2	315.67
2	0.50	0.2	296.15
3	0.75	0.2	299.16
4	1.00	0.2	308.31
5	1.50	0.2	320.38
6	0.25	0.3	291.33
7	0.50	0.3	275.43
8	0.75	0.3	277.04
9	1.00	0.3	280.73
10	1.50	0.3	298.92
11	0.25	0.4	285.36
12	0.50	0.4	271.74
13	0.75	0.4	276.16
14	1.00	0.4	280.95
15	1.50	0.4	292.84
16	0.25	0.5	306.64
17	0.50	0.5	292.74
18	0.75	0.5	294.63
19	1.00	0.5	302.79
20	1.50	0.5	309.40

are limited to W14 and W12 sections (Camp *et al.* 2005). In this example, the swarm size and the maximum number of iterations for MFO and EMFO algorithms are 20 and 150, respectively. In the optimization process, only the constraints given by Eqs. (4), (8) and (9) are checked. The results of sensitivity analysis are given in Table 1 indicating that the optimal setting of the internal parameters is  $\alpha = 0.5$  and  $\beta = 0.4$ .

In this study, the best results obtained by MFO and EMFO meta-heuristics are compared with those of found by GA (Pezeshk *et al.* 2000), ACO (Camp *et al.* 2005) and IACO (Kaveh and Talatahari 2010) in Table 2. The convergence histories of MFO and EMFO algorithms are compared in Fig. 3.

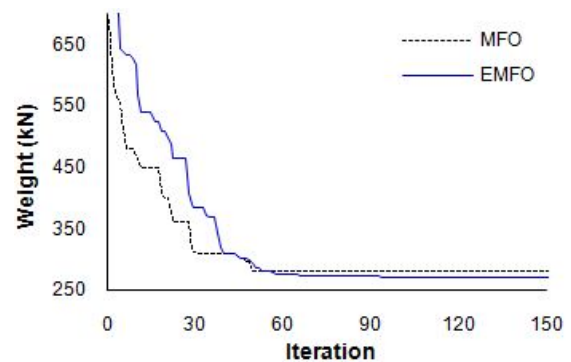


Fig. 3 Convergence histories of MFO and EMFO for ten-story planar steel frame

Table 2 Optimal designs of ten-story planar steel frame

Element groups	GA	ACO	IACO	Present work	
	(Pezeshk <i>et al.</i> 2000)	(Camp <i>et al.</i> 2005)	(Kaveh and Talatahari 2010)	MFO	EMFO
Beam 1-3S	W33×118	W30×108	W33×118	W30×108	W33×118
Beam 4-6S	W30×90	W30×90	W30×90	W30×90	W30×90
Beam 7-9S	W27×84	W27×54	W24×76	W24×84	W24×84
Beam 10S	W24×55	W21×44	W14×30	W21×62	W21×62
Column 1-2S	W14×233	W14×233	W14×233	W14×233	W14×211
Column 3-4S	W14×176	W14×176	W14×176	W14×159	W14×159
Column 5-6S	W14×159	W14×145	W14×145	W14×145	W14×145
Column 7-8S	W14×99	W14×99	W14×90	W14×90	W14×90
Column 9-10S	W12×79	W12×65	W12×65	W12×65	W12×58
Weight (kN)	289.72	278.48	274.99	280.78	271.89
Number of analyses	3690	8300	2500	3000	3000

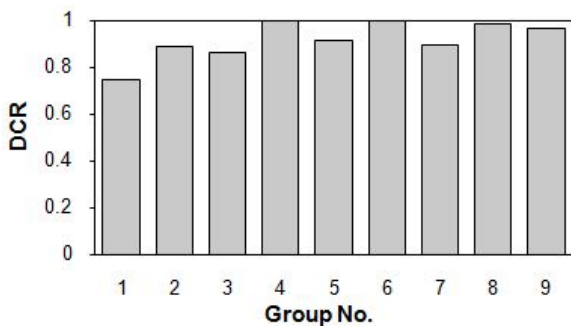


Fig. 4 Maximum DCR for each element group of optimal ten-story planar steel frame found by EMFO

The results indicate that the best solution found by EMFO is 6.15%, 2.37%, 1.13% and 3.17% lighter than those of obtained by GA, ACO, IACO and MFO, respectively. The proposed EMFO algorithm requires 3000 structural analyses to find an optimal solution which is less than the number of analyses required by GA and ACO and slightly more than the IACO. Furthermore, it can be observed from Fig. 3 that the EMFO has better convergence rate in comparison with MFO.

For the optimum design found by EMFO, the maximum DCR in element groups of the frame are depicted in Fig. 4. It can be observed that all DCRs are less than 1.0. Moreover, the maximum displacement of frame is 10.08 cm which is less than its limit of 12.47 cm. This means that the optimum solution is feasible and the DCR constraints dominate the design.

5.2 Three-bay twenty four-story planar steel frame

A twenty four-story frame and its element grouping details are shown in Fig. 5. The grouping results in 4 beam and 16 column sections for a total of 20 design variables. In this example,  $E = 205$  GPa,  $F_y = 230.3$  MPa,  $K_x \geq 1.0$  and  $K_y = 1.0$ . In this example the applied external loads are as:  $W = 25.628$  kN,  $w1 = 4.378$  kN/m,  $w2 = 6.362$  kN/m,  $w3 = 6.917$  kN/m and  $w4 = 5.954$  kN/m. The beams' sections are chosen from all W-shaped sections, while the section of

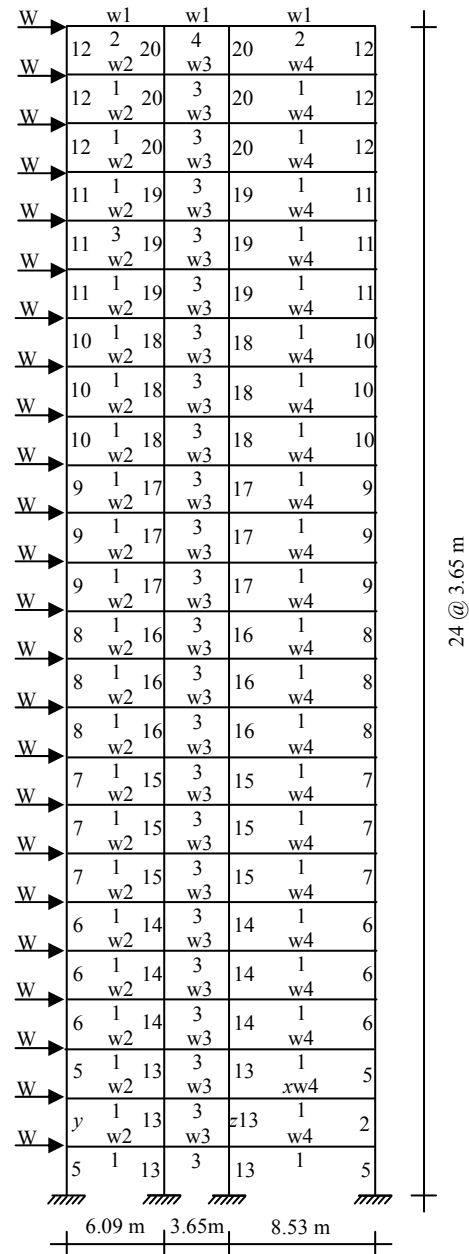


Fig. 5 Twenty four-story planar steel frame

Table 3 The results of sensitivity analysis for twenty four-story planar steel frame

No.	$\alpha$	$\beta$	Best weight (kN)
1	0.25	0.2	921.03
2	0.50	0.2	910.08
3	0.75	0.2	913.22
4	1.00	0.2	918.17
5	1.50	0.2	932.14
6	0.25	0.3	914.71
7	0.50	0.3	901.03
8	0.75	0.3	905.69
9	1.00	0.3	909.94
10	1.50	0.3	916.23
11	0.25	0.4	914.21
12	0.50	0.4	899.73
13	0.75	0.4	908.16
14	1.00	0.4	913.84
15	1.50	0.4	917.10
16	0.25	0.5	922.20
17	0.50	0.5	908.87
18	0.75	0.5	911.90
19	1.00	0.5	918.51
20	1.50	0.5	926.43

columns is limited to W14 sections. The maximum lateral displacement and maximum inter-story drift are limited to 29.2 and 1.217 cm, respectively. The size of swarm and the maximum number of iterations are 30 and 200, respectively. For the EMFO algorithm, the results of sensitivity analysis reported in Table 3 indicate that  $\alpha = 0.5$  and  $\beta = 0.4$  is the best setting of the internal parameters.

Table 4 compares the best designs found by MFO and EMFO with the solutions attained by HS (Degertekin 2010), TLBO (Togan 2012), DE (Kaveh and Farhodi 2013) and ES-DE (Talatahari *et al.* 2015). The results of Table 4 demonstrate that EMFO converges to an optimal solution which its weight is 5.69%, 0.15%, 1.16%, 4.60% and 2.45% less than those of HS, TLBO, DE, ES-DE and MFO, respectively.

In the framework of EMFO algorithm the optimum solution is obtained by conducting 6000 structural analyses which is considerably less than those of required by HS, TLBO and ES-DE algorithms. It is clear that the proposed EMFO meta-heuristic algorithm outperforms all the mentioned algorithms.

Fig. 6 shows the convergence histories of MFO and EMFO meta-heuristic algorithms indicating that the EMFO algorithm possesses better convergence behavior than the MFO.

The inter-story drifts and maximum DCR of each element group are respectively shown in Figs. 7 and 8 for the optimum design found by EMFO.

The results represented in Figs. 7 and 8 confirm the feasibility of the optimal design found by EMFO algorithm and reveal that the inter-story drift constraint is active in

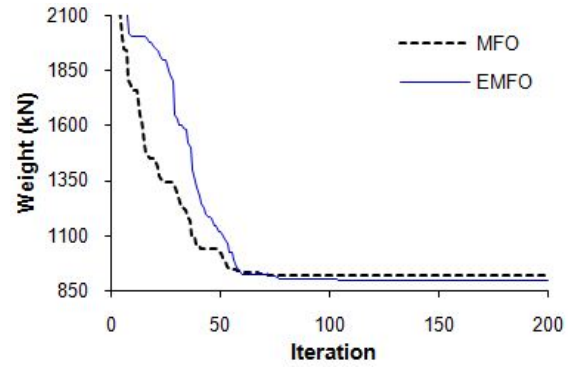


Fig. 6 Convergence histories of MFO and EMFO for twenty four-story planar steel frame

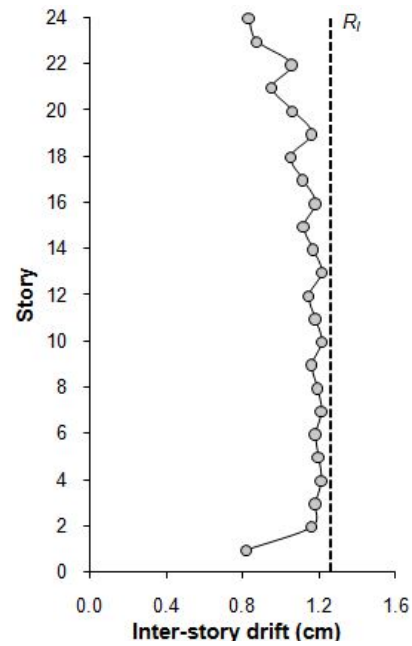


Fig. 7 Inter-story drifts for the optimal twenty four-story planar steel frame found by EMFO

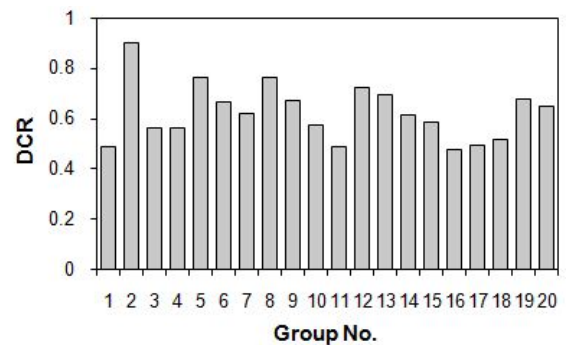


Fig. 8 Maximum DCR for each element group of optimal twenty four-story planar steel frame found by EMFO

this example.

### 5.3 Twenty-story 3D steel braced frame

The 3D and plan view of a twenty-story 3D steel braced

Table 4 Optimal designs of twenty four-story planar steel frame

Element groups	HS (Degertekin 2010)	TLBO (Togan 2012)	DE (Kaveh and Farhodi 2013)	ES-DE (Talatahari <i>et al.</i> 2015)	Present work	
					MFO	EMFO
1	W30×90	W30×90	W30×90	W30×90	W30×90	W30×90
2	W10×22	W8×18	W6×20	W21×55	W14×22	W14×22
3	W18×40	W24×62	W21×44	W21×48	W24×55	W21×48
4	W12×16	W6×9	W6×9	W10×45	W6×9	W6×9
5	W14×176	W14×132	W14×159	W14×145	W14×159	W14×145
6	W14×176	W14×120	W14×145	W14×109	W14×109	W14×120
7	W14×132	W14×99	W14×132	W14×99	W14×120	W14×109
8	W14×109	W14×82	W14×99	W14×145	W14×74	W14×74
9	W14×82	W14×74	W14×68	W14×109	W14×68	W14×68
10	W14×74	W14×53	W14×61	W14×48	W14×61	W14×61
11	W14×34	W14×34	W14×43	W14×38	W14×38	W14×48
12	W14×22	W14×22	W14×22	W14×30	W14×26	W14×22
13	W14×145	W14×109	W14×109	W14×99	W14×109	W14×109
14	W14×132	W14×99	W14×109	W14×132	W14×109	W14×109
15	W14×109	W14×99	W14×90	W14×109	W14×109	W14×99
16	W14×82	W14×90	W14×82	W14×68	W14×99	W14×99
17	W14×61	W14×68	W14×74	W14×68	W14×82	W14×74
18	W14×48	W14×53	W14×43	W14×68	W14×53	W14×53
19	W14×30	W14×34	W14×30	W14×61	W14×43	W14×30
20	W14×22	W14×22	W14×26	W14×22	W14×26	W14×22
Weight (kN)	956.13	903.02	912.26	945.15	924.31	901.70
Analyses	13924	12000	N/A	12000	6000	6000

frame with 960 elements are shown in Fig. 9. The columns in a story are divided into three member groups as corner, inner and outer columns. Also, beams are categorized into two groups as inner and outer beams. All the corner columns, inner columns, outer columns, inner beams, outer beams and bracings are grouped together as having the same section over two adjacent stories. Thus, there are 60 design variables in this example. The 3D steel braced frame is optimized following the AISC-ASD (1989) specification. Moreover, the displacements of all the joints in  $x$  and  $y$  directions are limited to 18.29 cm, and the upper limit of inter-story drifts is set to 0.91 cm. The geometric constraints are also included. The modulus of elasticity and yield stress are  $2.039 \times 10^{10}$  kg/m<sup>2</sup> and  $2.531 \times 10^7$  kg/m<sup>2</sup>, respectively. The dead and live loads acting on the first to 19th floors are equal to 2.88 kN/m<sup>2</sup> and 2.39 kN/m<sup>2</sup>, respectively. The roof is subjected to a dead load of 2.88 kN/m<sup>2</sup> and snow load of 1.20 kN/m<sup>2</sup>. The gravity loads are applied as uniformly distributed loads on the beams using distribution formulas developed for slabs by AISC-ASD (1989). The design wind loads are computed according to ASCE 7-05 (2005) using the following equation

$$p_w = (0.613K_zK_{zt}K_dV^2I)(GC_p) \quad (21)$$

where  $p_w$  is the design wind pressure in kN/m<sup>2</sup>,  $K_z$  is the velocity exposure coefficient,  $K_{zt}$  is the topographic factor,  $K_d$  is the wind direction factor,  $V$  is the basic wind speed,  $G$

is the gust factor and  $C_p$  is the external pressure coefficient. As specified by Hasancebi *et al.* (2011) assuming that the buildings are located in a flat terrain with  $V = 46.94$  m/s and exposure category B, the following values are used for these parameters:  $K_{zt} = 1.0$ ,  $K_d = 0.85$ ,  $I = 1.0$ ,  $G = 0.85$  and  $C_p = 0.8$  for windward face and 0.5 for leeward face.

The wind loads are applied as uniformly distributed lateral loads on the external beams located on windward and leeward facades at every floor level. The gravity and wind forces are combined under two loading conditions. In the first one, the gravity loads are applied with the wind loads acting along the  $x$ -axis, whereas in the second one, they are applied with the wind forces acting along the  $y$ -axis.

In this example, in order to implement optimization process, the swarm size is chosen to be 40 and the maximum number of iterations is limited to 500.

Table 5 represents the results obtained from the sensitivity analysis for the present example. As well as the previous examples, the best setting of the algorithmic parameters is  $\alpha = 0.5$  and  $\beta = 0.4$ .

The best optimal design found by MFO and EMFO are compared in Table 6 with the optimal designs obtained by ES (Hasancebi *et al.* 2011) and MPSO (Gholizadeh and Fattahi 2014). The results show that the optimum design attained by EMFO is 4.09%, 1.53% and 2.48% lighter than the designs obtained by ES, MPSO and MFO, respectively. It is clear that the computational demand of the EMFO, in

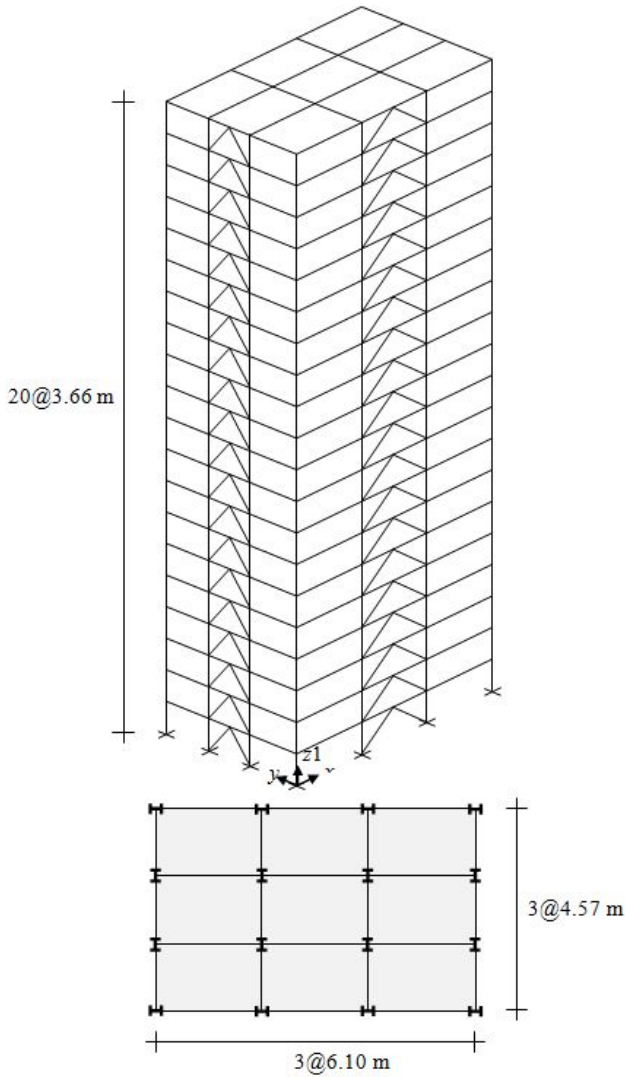


Fig. 9 Twenty-story 3D steel braced frame

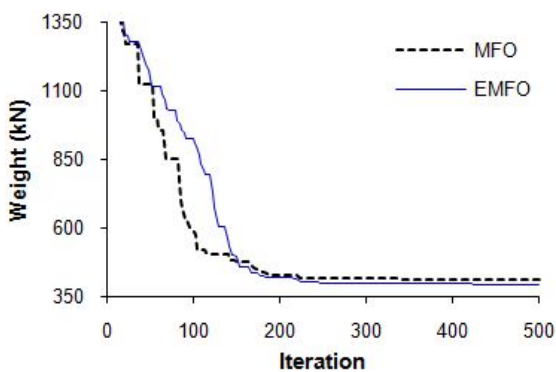


Fig. 10 Convergence histories of MFO and EMFO for twenty-story 3D steel braced frame

terms of required structural analyses, is equal to that of MPSO and significantly less than that of ES.

Comparison of convergence histories of MFO and EMFO algorithms in Fig. 10 demonstrates the better convergence rate of EMFO.

For the optimum design found by EMFO, the maximum

Table 5 The results of sensitivity analysis for twenty-story 3D steel braced frame

No.	$\alpha$	$\beta$	Best weight (kN)
1	0.25	0.2	419.13
2	0.50	0.2	407.52
3	0.75	0.2	411.31
4	1.00	0.2	414.75
5	1.50	0.2	421.36
6	0.25	0.3	406.63
7	0.50	0.3	398.86
8	0.75	0.3	401.23
9	1.00	0.3	404.01
10	1.50	0.3	409.49
11	0.25	0.4	407.50
12	0.50	0.4	396.03
13	0.75	0.4	403.04
14	1.00	0.4	404.47
15	1.50	0.4	410.32
16	0.25	0.5	417.82
17	0.50	0.5	406.41
18	0.75	0.5	410.22
19	1.00	0.5	413.65
20	1.50	0.5	420.68

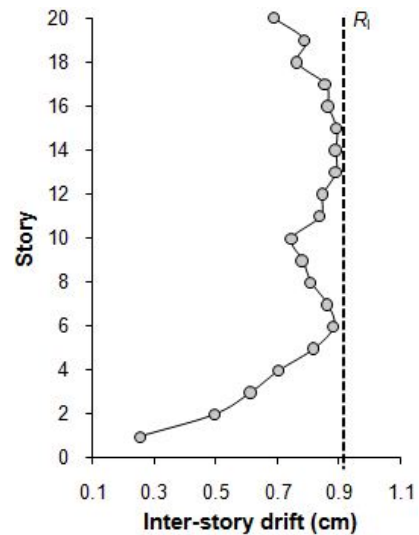


Fig. 11 Inter-story drifts for the optimal twenty four-story planar steel frame found by EMFO

lateral displacement is 13.80 cm, which is less than its allowable value of 18.29 cm. As the largest inter-story drift of this structure occurs in  $y$ -direction, the inter-story drift profile of the structure in this direction is depicted in Fig. 11. In addition, the maximum DCRs of the element groups are shown in Fig. 12. The results demonstrate the feasibility of the optimum design and show that both the inter-story drift and DCR constraints are active in this example.

## 6. Conclusions

MFO is one of the most recently developed algorithms based on the navigation method of natural moths and the

preliminary results demonstrate the efficiency of this algorithm compared to some existing algorithms for optimization of benchmark functions and a few benchmark truss structures. The popular optimization problem of steel

Table 6 Optimal designs of twenty-story 3D steel braced frame

Members	Story No.	Group No.	ES	MPSO	Present work	
			(Hasancebi <i>et al.</i> 2011)	(Gholizadeh and Fattahi 2014)	MFO	EMFO
Outer beam	1-2	1	W8×18	W10×22	W14×22	W10×22
	3-4	2	W10×22	W10×19	W6×20	W10×22
	5-6	3	W12×26	W10×19	W6×20	W10×22
	7-8	4	W18×35	W21×50	W18×50	W18×35
	9-10	5	W21×44	W21×68	W16×67	W21×68
	11-12	6	W12×26	W21×68	W16×67	W21×68
	13-14	7	W18×35	W16×31	W16×31	W18×35
	15-16	8	W16×36	W14×30	W12×30	W14×30
	17-18	9	W16×36	W16×57	W16×57	W16×57
	19-20	10	W10×33	W12×22	W10×22	W16×31
Inner beam	1-2	11	W24×62	W16×77	W16×77	W24×68
	3-4	12	W16×40	W24×62	W21×62	W24×62
	5-6	13	W30×108	W18×60	W18×60	W18×60
	7-8	14	W16×50	W24×62	W21×62	W24×62
	9-10	15	W16×50	W21×62	W24×62	W21×62
	11-12	16	W18×60	W16×40	W18×40	W18×35
	13-14	17	W21×44	W16×36	W16×36	W18×35
	15-16	18	W16×36	W16×26	W16×26	W16×31
	17-18	19	W14×34	W12×22	W10×22	W12×22
	19-20	20	W14×30	W12×22	W10×22	W14×22
Conner column	1-2	21	W12×106	W30×261	W44×262	W33×201
	3-4	22	W30×90	W33×221	W33×221	W33×201
	5-6	23	W18×97	W27×129	W27×129	W27×146
	7-8	24	W14×90	W24×104	W18×106	W24×104
	9-10	25	W14×109	W14×145	W24×146	W24×104
	11-12	26	W12×72	W14×145	W24×146	W21×132
	13-14	27	W14×90	W18×97	W18×97	W12×96
	15-16	28	W14×90	W18×97	W18×97	W12×96
	17-18	29	W10×39	W12×72	W14×74	W12×65
	19-20	30	W10×33	W8×31	W8×31	W10×33
Outer column	1-2	31	W14×233	W27×217	W33×221	W27×194
	3-4	32	W14×211	W27×178	W27×178	W27×161
	5-6	33	W14×211	W27×161	W24×162	W27×146
	7-8	34	W21×166	W18×175	W18×175	W24×162
	9-10	35	W14×132	W14×145	W24×146	W24×162
	11-12	36	W14×120	W27×94	W27×102	W18×97
	13-14	37	W12×106	W14×74	W14×74	W14×74
	15-16	38	W14×74	W14×68	W21×68	W14×68
	17-18	39	W12×58	W14×53	W14×53	W14×53
	19-20	40	W10×49	W6×20	W6×25	W8×31

Table 6 Continued

Members	Story No.	Group No.	ES	MPSO	Present work	
			(Hasancebi <i>et al.</i> 2011)	(Gholizadeh and Fattahi 2014)	MFO	EMFO
Inner column	1-2	41	W40×362	W30×235	W27×235	W33×221
	3-4	42	W40×268	W33×221	W33×221	W33×221
	5-6	43	W44×244	W27×217	W33×221	W27×217
	7-8	44	W44×244	W27×129	W27×129	W27×178
	9-10	45	W40×221	W30×99	W30×99	W27×161
	11-12	46	W40×149	W24×104	W24×104	W21×101
	13-14	47	W18×106	W18×106	W18×106	W21×101
	15-16	48	W30×99	W18×106	W18×106	W21×83
	17-18	49	W24×62	W21×50	W21×50	W21×50
	19-20	50	W16×36	W6×20	W6×25	W6×20
Bracing	1-2	51	W12×40	W8×31	W8×31	W8×31
	3-4	52	W8×40	W8×31	W8×31	W8×31
	5-6	53	W8×31	W12×26	W8×31	W12×26
	7-8	54	W12×26	W8×24	W8×24	W6×25
	9-10	55	W6×20	W8×24	W8×24	W6×25
	11-12	56	W10×22	W8×18	W8×18	W8×18
	13-14	57	W6×15	W8×18	W5×19	W5×19
	15-16	58	W6×15	W8×18	W5×19	W8×18
	17-18	59	W4×13	W4×13	W5×19	W4×13
	19-20	60	W4×13	W4×13	W4×13	W4×13
Weight (ton)			412.91	402.2	406.13	396.03
Analyses			60000	20000	20000	20000

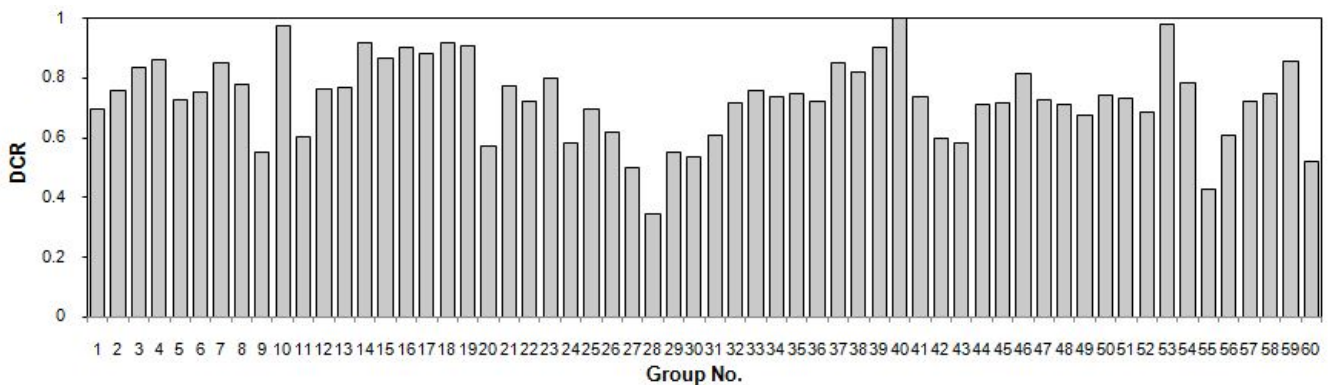


Fig. 12 Maximum DCR for each element group of optimal twenty-story 3D steel braced frame found by EMFO

frame structures is tackled in the present work and the numerical results demonstrate that the MFO could not show superior performance as compared to other algorithms. Therefore the main objective of this study is to enhance the performance of the MFO algorithm for solving the optimization problem of steel frame structures by proposing an enhanced MFO (EMFO) algorithm.

In order to achieve this task, a new equation is employed for position updating based on the best information derived by the search agents during the optimization process. Furthermore, a mutation operator is added to the algorithm

to decrease the probability of trapping into local optimal designs.

The efficiency of the proposed EMFO algorithm is illustrated by presenting three benchmark size optimization problems of steel frame structures with discrete design variables. The results obtained by EMFO in all examples are compared with the optimum designs found by MFO and other algorithms. The first example of this study is a 2D one-bay ten-story steel frame with 9 design variables and the EMFO finds the best weight for this frame which is respectively 6.15%, 2.37%, 1.13% and 3.17% less than

those of the GA, ACO, IACO and MFO algorithms at almost the same computational effort. As the second example, a three-bay twenty four-story planar steel frame with 20 design variables is optimized and the results show that the EMFO converges to an optimum design which its weight is 5.69%, 0.15%, 1.16%, 4.60% and 2.45% lighter than those of HS, TLBO, DE, ES-DE and MFO algorithm, respectively at less computational effort. Finally, the EMFO algorithm is employed to tackle the optimization problem of a twenty-story 3D steel braced frame structure with 60 design variables. In this example, the optimum solution obtained by EMFO is 4.09%, 1.53% and 2.48% lighter in comparison with the ES, MPSO and MFO, respectively at less computational demand.

As it can be seen in convergence curves of Figs. 3, 6, and 10, in the first half of the optimization process the mutation helps to increase the exploration ability of EMFO compared to standard MFO. On the other hand, elitism (via the proposed equation for position updating) makes that exploitation characterizes the last half of the optimization process and this helps the EMFO algorithm to not get stuck at local optima.

The numerical results imply that the proposed EMFO meta-heuristic algorithm not only converges to better optimal solutions compared to the mentioned meta-heuristic algorithms but it also requires less structural analyses during its search process. Consequently, the proposed EMFO meta-heuristic can be efficiently utilized to tackle the discrete optimization problem of steel moment resisting frame and steel braced frame structures with large number of design variables.

## References

- AISC-ASD (1989), American Institute of Steel Construction-Allowable Stress Design; Manual of Steel Construction, (9th Ed.), Chicago, IL, USA.
- AISC-LRFD (2001), American Institute of Steel Construction-Load and Resistance Factor Design; Manual of steel construction, Chicago, IL, USA.
- ANSYS Incorporated (2006), ANSYS Release 10.0.
- Artar, M. and Daloğlu, A.T. (2015), "Optimum design of composite steel frames with semi-rigid connections and column bases via genetic algorithm", *Steel Compos. Struct., Int. J.*, **19**(4), 1035-1053.
- ASCE 7-05 (2005), Minimum design loads for building and other structures.
- Aydin, E., Sonmez, M. and Karabork, T. (2015), "Optimal placement of elastic steel diagonal braces using artificial bee colony algorithm", *Steel Compos. Struct., Int. J.*, **19**(2), 349-368.
- Camp, C.V., Bichon, B.J. and Stovall, S.P. (2005), "Design of steel frames using ant colony optimization", *J. Struct. Eng.*, **131**(3), 369-379.
- Degertekin, S.O. (2008), "Optimum design of steel frames using harmony search algorithm", *Struct. Multidisc. Optim.*, **36**(4), 393-401.
- Gholizadeh, S. and Fattahi, F. (2014), "Design optimization of tall steel buildings by a modified particle swarm algorithm", *Struct. Des. Tall Spec. Buil.*, **23**(4), 285-301.
- Gholizadeh, S. and Barati, H. (2014), "Topology optimization of nonlinear single layer domes by a new metaheuristic", *Steel Compos. Struct., Int. J.*, **16**(6), 681-701.
- Gholizadeh, S. and Poorhoseini, H. (2015), "Optimum design of steel frame structures by a modified dolphin echolocation algorithm", *Struct. Eng. Mech., Int. J.*, **55**(3), 535-554.
- Hasancebi, O., Bahcecioglu, T., Kurc, O. and Saka, M.P. (2011), "Optimum design of high-rise steel buildings using an evolution strategy integrated parallel algorithm", *Comput. Struct.*, **89**(21), 2037-2051.
- Kaveh, A. and Bakhshpoori, T. (2015), "Subspace search mechanism and cuckoo search algorithm for size optimization of space trusses", *Steel Compos. Struct., Int. J.*, **18**(2), 289-303.
- Kaveh, A. and Farhoudi, N. (2013), "A new optimization method: Dolphin echolocation", *Adv. Eng. Softw.*, **59**, 53-70.
- Kaveh, A. and Shokohi, F. (2015), "Optimum design of laterally-supported castellated beams using CBO algorithm", *Steel Compos. Struct., Int. J.*, **18**(2), 305-324.
- Kaveh, A. and Talatahari, S. (2010), "An improved ant colony optimization for the design of planar steel frames", *Eng. Struct.*, **32**(3), 864-873.
- Lamberti, L. and Pappalettere, C. (2011), "Metaheuristic design optimization of skeletal structures: a review", *Comput. Technol. Rev.*, **4**(1), 1-32.
- MATLAB (2006), The language of technical computing; The Math Works. [Software]
- Mirjalili, S. (2015), "Moth-flame optimization algorithm: A novel nature-inspired heuristic paradigm", *Knowl.-Based. Syst.*, **89**, 228-249.
- Pezeshk, S., Camp, C.V. and Chen, D. (2000), "Design of nonlinear framed structures using genetic algorithms", *J. Struct. Eng.*, **126**(3), 382-388.
- Rafiee, A., Talatahari, S. and Hadidi, A. (2013), "Optimum design of steel frames with semi-rigid connections using Big Bang-Big Crunch method", *Steel Compos. Struct., Int. J.*, **14**(5), 431-451.
- Talatahari, S., Gandomi, A.H., Yang, X.S. and Deb, S. (2015), "Optimum design of frame structures using the eagle strategy with differential evolution", *Eng. Struct.*, **91**, 16-25.
- Togan, V. (2012), "Design of planar steel frames using teaching-learning based optimization", *Eng. Struct.*, **34**, 225-232.

CC